Nuclear Engineering and Technology 55 (2023) 640–647

Contents lists available at ScienceDirect

Nuclear Engineering and Technology

journal homepage: www.elsevier.com/locate/net

Original Article

Dependence of Na^+ leakage on intrinsic properties of cation exchange resin in simulated secondary environment for nuclear power plants

Hyun Kyoung Ahn, Chi Hyun An, Byung Gi Park, In Hyoung Rhee*

Department of Energy & Environment Engineering, Soonchunhyang University, Chungche Songnam-do, Republic of Korea

ARTICLE INFO

Article history:
Received 7 February 2022
Received in revised form
10 October 2022
Accepted 16 October 2022
Available online 20 October 2022

Keywords:
Ion exchange
Leakage
Selectivity
Size
Void
Resin layer

ABSTRACT

Material corrosion in nuclear power plant (NPP) is not controlled only by amine injection but also by ion exchange (IX) which is the best option to remove trace Na^+. This study was conducted to understand the Na^+ leakage characteristics of IX beds packed with ethanolamine-form (ETAH-form) and hydrogen-form (H-form) resins in the simulated water-steam cycle in terms of intrinsic behaviors of four kinds of cation-exchange resins through ASTM test and Vanselow mass action modeling. Na^+ was inappreciably escaped throughout the channel created in resin layer. Na^+ leakage from IX bed was non-linearly raised because of its decreasing selectivity with increasing Na^+ capture and with increasing the fraction of ETAH-form resin. Na^+ did not reach the breakthrough earlier than $ETAH^+$ and NH_4^+ due to the increased selectivity of Na^+ to the cation-exchange resin ($H^+ < ETAH^+ < NH_4^+ \ll Na^+$) at the feed composition. Na^+ leakage from the resin bed filled with small particles was decreased due to the enhanced dynamic IX processes, regardless of its low selectivity. Thus, the particle size is a predominant factor among intrinsic properties of IX resin to reduce Na^+ leakage from the condensate polishing plant (CPP) in NPPs.

1. Introduction

The corrosion of the material in the water-steam cycle of nuclear power plant (NPP) is reduced by purifying the circulating solution through ion exchange (IX) and by maintaining the weakly basic environment through the injection of amine such as ethanolamine (ETA) and ammonia (NH_3) [1–3]. Every ionic chemical including amine species is supposed to be almost completely removed with ion exchange resin. The complete removal of such ions as Na^+Cl^- negligibly present in each circulation should be desirable, while the amine injected in each circulation is not necessarily eliminated. A trace amount of Na^+ may be introduced into the system water of NPP by the insufficient removal during the generation of pure water, the incomplete elimination by the purification system, the contamination caused by repair works, the injection of chemical additives including impurities, and the leak of seawater in condenser [4–7].

The leakage of a trace of Na^+ is higher from IX bed filled with ethanolamine-form (R-ETAH) than with hydrogen-form (R–H) resin and is not represented by the typical pattern of breakthrough for major components [8]. The minor component, e.g., trace Na^+, does not come close to the breakthrough even long after the breakthrough of major component after which its leakage is nevertheless gradually increased [8]. The amine-saturated IX resin, which does not remove amine selectively, is ideally suitable for the water-steam circulation system in NPP [2]. The amine-saturated operation of IX bed in condensate polishing plant (CPP) is preferred in terms of the extension of life span for CPP operation, the saving of chemical for pH control, and the reduction of waste-water discharge for resin regeneration. However, the increased Na^+ leakage from ion-exchange beds in amine-saturated operation has been the big predicament for its introduction into NPP.

In general, ion exchange is fast possibly because no bonding electron-pairs need to be broken and however, the rate of IX process is remarkably limited by the rate of ion diffusion in and out of the exchanger structure. The IX process may be enhanced for the ions with higher diffusion rate, for the exchanger with the larger openness of its structure, and for higher strength interacting between exchanger and ions [9,10]. The degree of the openness is influenced by the swelling rate and the water content of an exchanger, while the affinity depends on the inherent property of ion and exchanger, ionic strength and composition, and the ion mole fraction in the solution and solid phases. Ion exchange column is a complicated non-equilibrium system interpreted by the

* Corresponding author.
E-mail address: ihrhee@sch.ac.kr (I.H. Rhee).

https://doi.org/10.1016/j.net.2022.10.018

Nomenclature

K	Selectivity constant
k	Selectivity coefficient
X	Mole fraction
γ	Activity coefficient in the solution phase
$k_{R\text{-}Na}$	Average selectivity coefficients of Na^+
$k_{R\text{-}NH4}$	Average selectivity coefficients of NH_4^+
$k_{R\text{-}ETAH}$	Average selectivity coefficients of $ETAH^+$

equilibrium distribution by ion exchange, the rate of mass transfer, and the statistical variations in the flow paths between the exchanger structures. Those phenomena may deteriorate the IX process of mobile ions which are fast pushed down the column at the steady flow of solution.

The objective of this study is to understand the characteristics on Na leakage from the IX bed with physical and chemical behaviors of IX resins in the simulated water-steam cycle of mixed ammonia and ethanolamine solution including a small amount of Na^+. The intrinsic properties were obtained with test apparatuses and procedures according to American Society for Testing Materials (ASTM), while the selectivity of IX resin to ions was determined with equilibrium batch test by applying Vanselow IX equation. The semi-action modeling for binary cation exchange was fulfilled to evaluate the versatility of ion selectivity.

2. Experimentals and methods

The test procedure of ASTM [11] was applied to examine the intrinsic properties of four kinds of cation-exchange resins including cation exchange capacity, density, size, and uniformity. The semi-mass action model of Vanselow equation was meanwhile adopted to quantify the cation selectivity of resins for H^+, Na^+, NH_4^+, and $ETAH^+$ using the experimental data collected from the batch test for IX equilibrium. The chemical analyses were carried out using acid-base titration (848 Titrino plus, Metrohm), spectroscopy (AA-7000, SHIMADZU), and ion chromatography (AT3000, FUTECS).

The review and analyses on the previous work [8] were performed to investigate Na^+ leakage from the mixed (cation and anion) IX beds of H- and ETAH-form resins at 20, 200, and 1000 ppb Na^+ in influent. The cation mole fraction of the feed solution at pH 10 comprises the major components of ~46% NH_4^+ (2.45×10^{-4} eq/L) and ~54% $ETAH^+$ (2.90×10^{-4} eq/L) and the minor component of Na^+ at 0.064 (20), 0.64 (200), and 3.2% (1000 ppb).

2.1. Intrinsic properties of strong acid cation-exchange resin

Four kinds of strong acid cation-exchange resins, one of which is world widely used in NPP (resin A), were selected, pretreated, and tested to investigate the moisture content, backwashed & settled density, particle size distribution, and total cation exchange capacity according to ASTM procedure [11]. Cation exchange resin was converted to hydrogen-form by backwashing the resin with pure water, followed by saturation of the cation-exchange resin with (1 + 9) HCl solution and then backwashing with pure water until pH 3.9 or higher. As shown in Table 1, resin A and B are gel-type, while resin C and D are MR-type (Macro Reticular).

Water retention capacity as a unit of percent is generally related to pore volume and determined from the loss of mass on drying at 104 ± 2 °C. The numerical value is dependent on functionality, polymer type, effective crosslinking, ionic form, and fouling. Backwashed & settled density as a unit of g/mL is calculated from the settled volume (mL) of ion-exchange material with the given mass (grams) which is added, backwashed, partially drained and settled in the operating IX bed. Particle size and distribution are decided from the volume retained (for 40 and 90% of samples) in water with a series of standard sieves of progressively decreasing size of opening (2.36 mm–150 μm). The effective size is the sieve opening in millimeters that retains 90% of the sample and the uniformity coefficient is the ratio of retaining 40%–90% of the sample in mesh size. Total cation exchange capacity, total number of exchangeable hydrogens in the cation-exchange resin as a unit of milliequivalents, is determined from the equilibration of the hydrogen-form resin within a known excess of standard sodium hydroxide solution in the presence of sodium chloride, followed by titration of the residual hydroxide ion with standard acid solution.

Backwashed & settled density and total cation exchange capacity were not much different for four kinds of IX resins, while the moisture content and uniformity coefficient were lower for gel-type than MR-type resins. The effective size was smallest for resin B and largest for resin A.

2.2. Selectivity determination with Vanselow Equation

The equilibrium batch tests for binary cation exchange on the four kinds of strong acid cation exchange resin involving H^+, Na^+, NH_4^+, and $ETAH^+$ were fulfilled in the chloride background over the medium range of concentrations to calculate the selectivity coefficients of cations with Vanselow equation.

As shown below, binary cation exchange between H^+ in the solid phase (R-) and M^+ in the solution phase is described and mass action equation of Vanselow is defined, in which parenthesis (·), bracket [·], and X are activity, concentration, and mole fraction, respectively.

Cation Exchange Reaction (M^+: Na^+, NH_4^+, $ETAH^+$)

$$R{-}H + M^+ \leftrightarrows R\text{-}M + H^+ \tag{1}$$

$$R^- + H^+ \leftrightarrows R - H \;\; ; \;\; k_{R-M} = 1 \tag{2}$$

$$R^- + M^+ \leftrightarrows R - M \;\; ; \;\; k_{R-M} \tag{3}$$

$$ETA\ (ethanolamine) + H_2O \leftrightarrows ETAH^+ + OH^-;\ K_b = 10^{-4.5} \tag{4}$$

$$NH_3\ (ammonia) + H_2O \leftrightarrows NH_4^+ + OH^-;\ K_b = 10^{-4.8} \tag{5}$$

Selectivity Constant (Thermodynamic Equilibrium Constant)

$$K = \frac{(R-M)(H^+)}{(R-H)(M^+)} \tag{6}$$

Selectivity Coefficient for Vanselow Equation

$$k_v = \frac{k_{R-M}}{k_{R-H}} = k_{R-M} = \frac{X_{R-M}\,(H^+)}{X_{R-H}\,(M^+)} = \frac{X_{R-M} \times \gamma_{H^+} \times [H^+]}{X_{R-H} \times \gamma_{M^+} \times [M^+]} \tag{7}$$

Since the activity of cation in the solid phase is not established, thermodynamic equilibrium constant for ion exchange reaction, i.e., selectivity constant, cannot be universally determined. Instead of selectivity constant (K), selectivity coefficient (k) is widely used, where the activity of cation in the solid phase is replaced with molarity, equivalent, mole fraction (X), equivalent fraction, and so on. The activity coefficient in the solution phase (γ) mainly depends on total ionic concentration. Selectivity is more consistent for binary cation exchange between mono-valent cations than between mono-/di-valent cations in the wide range of concentration [12].

Table 1
Types and characteristics of strong acid cation exchange resins (at 25 °C).

Properties of resin	Type of resin			
	Resin A	Resin B	Resin C	Resin D
DVB(divinyl benzene)[a]	16%, Gel	16%, Gel	18%, MR	20%, MR
Backwashed & settled density (g/mL)	1.93	1.65	1.81	1.85
Effective size (diameter, μm)	602	429	520	545
Uniformity coefficient	1.07	1.07	1.23	1.24
Total cation exchange capacity (meq/g dried)	4.16	4.28	4.62	4.42

[a] Product data sheet.

Numerical values of selectivity coefficient for H^+, Na^+, NH_4^+, and $ETAH^+$ were determined on the same total cation concentration in the liquid and resin phases of 0.05 N. R–H resin equivalent to the concentration of 0.05 N was added into 5 different combinations of 100 mL with 0.05 N H^+Cl^- and 0.05 N Na^+Cl^- solutions for binary cation exchange between H^+ and Na^+. Instead of Na^+Cl^-, 0.05 N $NH_4^+Cl^-$ and $ETAH^+Cl^-$ solutions were used for H^+/NH_4^+ and $H^+/ETAH^+$ binary cation exchanges. The concentrations of H^+ and $Na^+/NH_4^+/ETAH^+$ were measured in the solution and resin phases after the equilibration of 16 h with agitation and the respective mole fractions of $Na^+/NH_4^+/ETAH^+$ over H^+ were calculated and are represented in Fig. 1 for resin A, B, C and D. The selectivity coefficients over 5 samples were calculated with Vanselow equation for H–Na, H–NH_4 and H-ETAH binary cation exchanges on four kinds of resins and was arithmetically averaged, which is presented as the range and average values in Table 2.

Based on R–H resin, the selectivity of resin A, B, C, and D to Na^+, NH_4^+, and $ETAH^+$ were not identical but in the order of $NH_4^+ > Na^+ > ETAH^+ > H^+$ for binary cation exchange. The affinity of IX resin was decreased in the order of resin C ≥ A ≫ D > B for Na^+, NH_4^+, and $ETAH^+$. Cation selectivities were smallest for resin B and biggest for resin C. The average selectivity coefficients of Na^+, NH_4^+, and $ETAH^+$ ($k_{R\text{-}Na}$, $k_{R\text{-}NH4}$, $k_{R\text{-}ETAH}$) were equal to 1.83, 2.25, 1.65 for resin B and 2.43, 3.14, 2.31 for resin C, as shown in parenthesis in Table 2 when the selectivity coefficient of the resin to H ($k_{R\text{-}H}$) is assigned to be 1. The calculated selectivity coefficient of cation was not constant over the test range of its fraction in the solution which was relatively higher at the lower fraction in the solution and in the resin phases.

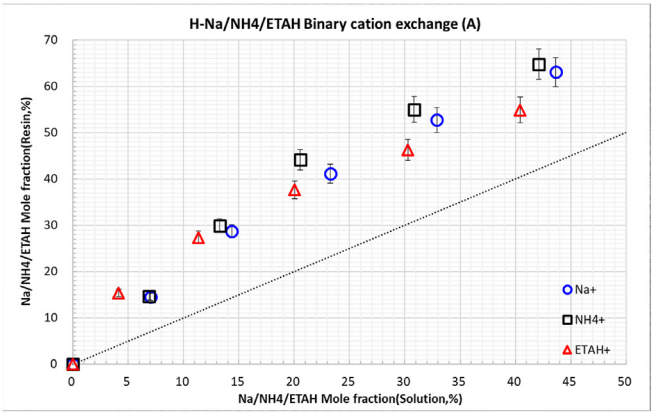

(a) Cation exchange on resin A

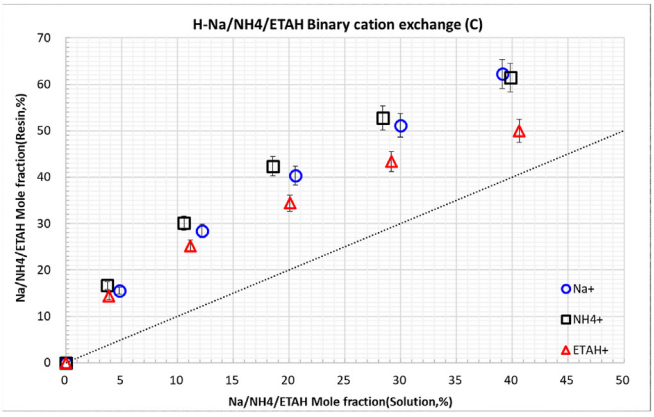

(c) Cation exchange on resin C

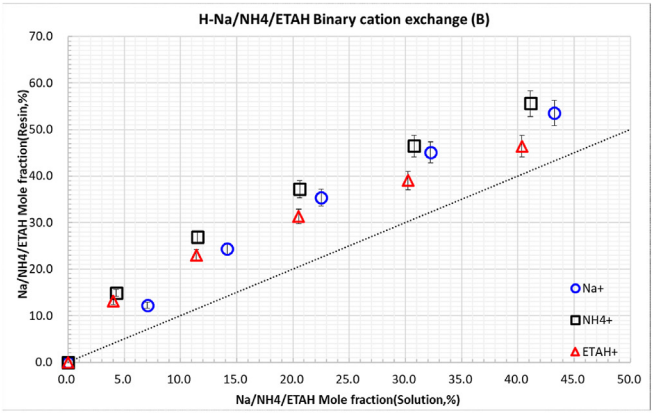

(b) Cation exchange on resin B

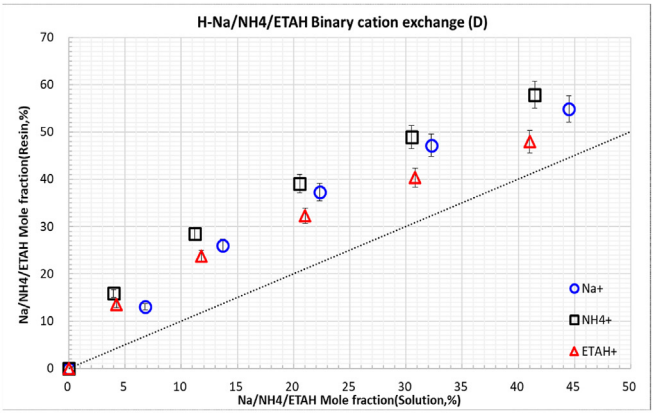

(d) Cation exchange on resin D

Fig. 1. Binary cation exchanges of H^+/Na^+, H/NH_4^+, and $H^+/ETAH^+$ on 4 different resins (at 25 °C).

Table 2
Selectivity coefficient for cation exchange reaction R–H + M^+ = R-M + H^+ (at 25 °C).

Cation exchange	Type of resin			
	A	B	C	D
H–Na	2.40–2.21 (2.43 ± 0.12)	1.96–1.51 (1.83 ± 0.09)	3.67–2.57 (2.68 ± 0.13)	2.21–1.52 (2.06 ± 0.10)
H–NH_4	3.06–2.32 (3.14 ± 0.16)	3.89–1.79 (2.25 ± 0.13)	5.20–2.41 (3.25 ± 0.16)	4.54–1.94 (2.50 ± 0.13)
H-ETAH	4.21–1.80 (2.31 ± 0.12)	3.59–1.28 (1.65 ± 0.08)	4.21–1.46 (2.12 ± 0.11)	3.53–1.32 (1.70 ± 0.09)

(·): mean value.

3. SEMI-MASS action modeling with Vanselow equation

Vanselow equation was applied to the experimental data obtained from R-ETAH resin for binary cation exchange between $ETAH^+$ and $H^+/Na^+/NH_4^+$ on 4 resins in the chloride background over the medium range of concentrations to test the reversible and predicting abilities of cation selectivity coefficients.

The reversibility of cation exchange reaction was evaluated by determining the selectivity coefficients of Na^+, NH_4^+, and $ETAH^+$ based on R-ETAH resin, which was subsequently compared with those previously obtained from R–H resin in Table 2. R-ETAH resin equivalent to the concentration of 0.05 N was added into 5 different combinations of 100 mL with 0.05 N $ETAH^+Cl^-$ and 0.05 N $H^+Cl^-/Na^+Cl^-/NH_4^+Cl^-$ solutions for binary cation exchange between $ETAH^+$ and $Na^+/NH_4^+/H^+$. The mean values of selectivity coefficients of Na^+, NH_4^+, and $ETAH^+$ ($k_{R\text{-}Na}$, $k_{R\text{-}NH4}$, $k_{R\text{-}ETAH}$) were 1.11, 1.36, 0.61 for resin B and 1.26, 1.53, 0.47 for resin C, as shown in brackets in Table 3, after normalization with $k_{R\text{-}H} = 1$. The selectivity coefficients based on R-ETAH were not the same as those determined from R–H resin, even for binary cation exchange between monovalent cations on commercial synthetic ion exchange resin of the well-known structure and thereby the mole fraction is not still enough to be substituted for the activity in the solid phase.

Semi-mass action modeling with Vanselow equation for resin A, B, C, and D was performed by applying mean values of the selectivity coefficients determined from R–H resin (Table 2) to the data of binary cation exchange obtained from R-ETAH resin, as illustrated in Fig. 2. As shown in Table 3, ion selectivity was diminished with increasing the coverage of cation in the solid phase and was not constant over the medium range of concentration. Overall, Vanselow equation yields the limited accuracy in predicting binary cation exchange on 4 resins in which the fitting is relatively better for resin B. It suggests that the deviation of cation selectivity is small for resin B over the given concentration range, as compared with resin A, C, and D, and the bigger the selectivity variation the worse the fitting.

4. Na^+ leakage from ion-exchange resin bed

The characteristics of trace Na leakage from IX bed was correlated with the chemical property including the selectivity as well as physical properties such as particle size, porosity, and void volume to obtain the mechanistic insights into the leakage phenomena. The review and analyses on Na leakage were performed with the experimental data with mixed-IX beds of H- and ETAH-form resins which were obtained by injecting the combined ammonia (2.45×10^{-4} eq/L) and ethanolamine (2.90×10^{-4} eq/L) solution at pH 10, where Na^+ were included at 20 (0.064), 200 (0.64), and 1000 (3.2%) ppb in concentration.

4.1. Overview on Na^+ leakage characteristics

Na^+ leakage from IX bed needs to be interpreted by its magnitude before and after BT (Breakthrough Time) of major component, its reliance on the incoming Na^+ concentration, and its variation with the kinds of IX resins, based on the following experimental observation [8].

1 **Leakage trend**: Na^+ at bed outlet was present inconsiderably and significantly, respectively before and after the BT point of major component. But Na^+ was not reached to its complete saturation in the resin layer after more than 3 times the BT of major component. It means that the selectivity of Na^+ to IX resin should be much higher relative to NH_4^+ and $ETAH^+$.
2 **Incoming Na^+concentration** (ionic strength and mole fraction): Na^+ leakage from cation-exchange resin becomes earlier and greater at the higher concentration of NaCl at bed inlet.
3 **Kinds of cation-exchange resins**: Na^+ leakage was not identical for 4 kinds of cation-exchange resins.

The feed solution with the major components of ETA and NH_3 and a minor component of NaCl at pH 10 was added into the mixed-bed of H- and ETAH-form resins which consisted of cation-exchange resin A and B with common anion-exchange resin. The amounts of Na^+ released from IX beds were shown at the incoming

Table 3
Selectivity coefficient for cation exchange reaction R-ETAH + M^+ = R-M + $ETAH^+$ (at 25 °C).

Cation exchange	Type of resin			
	A	B	C	D
ETAH-H	1.06–0.53 (0.43 ± 0.02) →[2.31 ± 0.12]	0.83–0.40 (0.61 ± 0.03) →[1.65 ± 0.08]	0.96–0.46 (0.47 ± 0.02) →[2.12 ± 0.11]	0.90–0.53 (0.59 ± 0.03) →[1.70 ± 0.09]
ETAH-Na	1.45–0.81 (1.05 ± 0.05) →[2.43 ± 0.12]	1.16–0.63 (1.11 ± 0.06) →[1.83 ± 0.09]	2.06–0.86 (1.26 ± 0.06) →[2.68 ± 0.13]	1.48–0.75 (1.21 ± 0.06) →[2.06 ± 0.10]
ETAH-NH_4	2.83–1.03 (1.36 ± 0.07) →[3.14 ± 0.16]	2.02–0.81 (1.36 ± 0.07) →[2.25 ± 0.13]	3.56–1.07 (1.53 ± 0.08) →[3.25 ± 0.16]	3.53–1.02 (1.47 ± 0.07) →[2.50 ± 0.13]

( ): mean value based on $k_{R\text{-}ETAH} = 1$. [ ]: normalized value, based on $k_{R\text{-}H} = 1$.

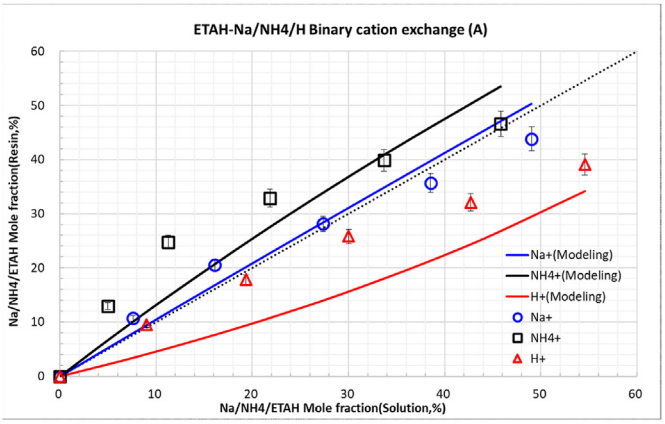

(a) Cation exchange on resin A

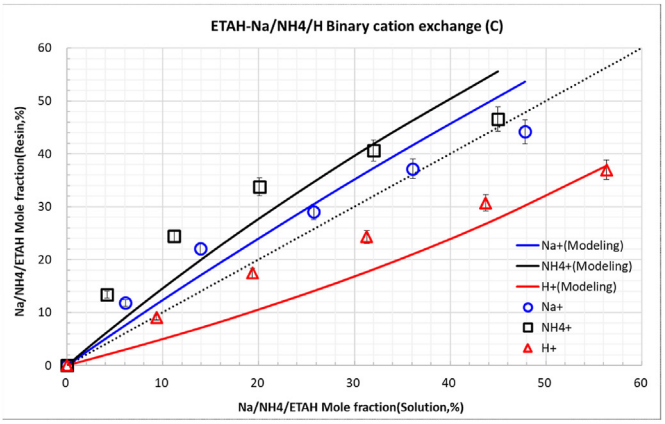

(c) Cation exchange on resin C

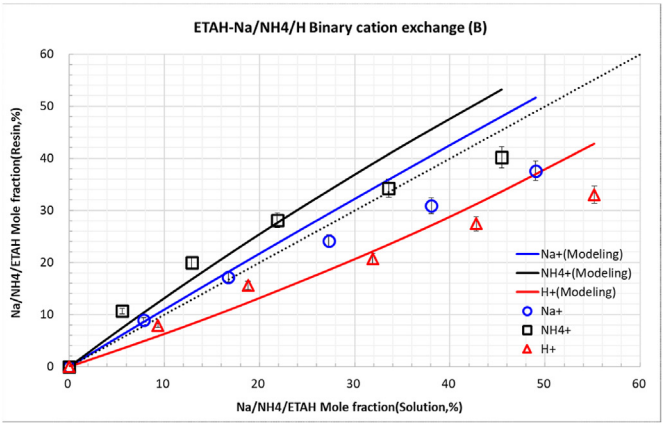

(b) Cation exchange on resin B

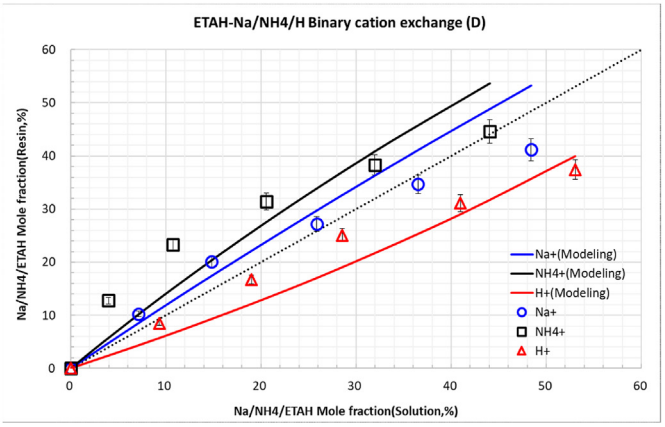

(d) Cation exchange on resin D

Fig. 2. Binary cation exchanges of $ETAH^+/Na^+$, $ETAH^+/NH_4^+$, and $ETAH^+/H^+$ on 4 different resins (at 25 ℃).

Na^+ concentration of 20, 200, and 1000 ppb in Fig. 3. The leakage of the minor component (Na^+) from the IX bed was decreased before the beginning BT and increased during BT of main components for the higher concentration of Na^+ at bed inlet. As compared with resin B, Na^+ leakage from IX bed filled with resin A at 20 ppb Na^+ in influent was higher by 0.83% and 3.95%, respectively before the beginning and during BT of main component, irrespective of the higher selectivity of Na^+ to resin A than to resin B, as illustrated in Table 2. It was also higher for ETAH-form resin than for H-form resin due to the lower selectivity of Na^+ to $ETAH^+$ to H^+.

4.2. Dependence of Na^+ leakage on chemical property of resin (selectivity)

4.2.1. Effect of solution composition on Na^+ selectivity and BT curve

As mentioned in section 2.2, the average ion-selectivity of four kinds of H-form cation-exchange resins to ions were decreased in the order of $NH_4^+ > Na^+ > ETAH^+ > H^+$. However, the selectivity of the minor component (Na^+) is especially increased because Na^+ is in the lower range of mole fraction in the liquid and resin phases. As shown in Fig. 2 (b), the individual ion-selectivity coefficient for resin B is < 1.8 for NH_4^+, < 1.3 for $ETAH^+$, and > 2 for Na^+ when the cation mole fraction of the feed solution is ~54% for $ETAH^+$, ~46% for NH_4^+ and <5% for Na^+. That is, the individual ion-selectivity is decreased in the order of $Na^+ > NH_4^+ > ETAH^+ > H^+$. The BT sequence is subsequently changed or reversed for the solution components and Na^+ may be under-saturated even after the BT of major components. In addition, the affinity of Na^+ to resin is higher for resin A than for resin B (resin $C \geq A \gg D > B$), which cannot account for the larger leakage of Na^+ from IX bed filled with resin A than with resin B.

Since the IX column is a non-equilibrium kinetic system, the point/pattern of BT relies on characteristics of ion such as selectivity and diffusivity, the properties of resin such as openness and void, flow rate and retention time, and column geometry [13–15]. The ideal ion exchange between ions with the same selectivity is represented as step-input behaviors for BT at the same point, while the competitive IX between ions with the different selectivity is demonstrated as S-shaped curves for BT at the correspondingly different points. The BT sequence in multi-component solution is determined by the selectivity for every component that varies with ionic strength and the fraction in the feed solution, besides cation exchange capacity. Those properties were evaluated by the concept of the relative selectivity of ion determined from the BT width in BT curve [8].

At the higher concentration of a minor component, the major component (NH_4^+ and $ETAH^+$) becomes earlier at the BT point and broader in the BT zone (due to the net reduced selectivity) because

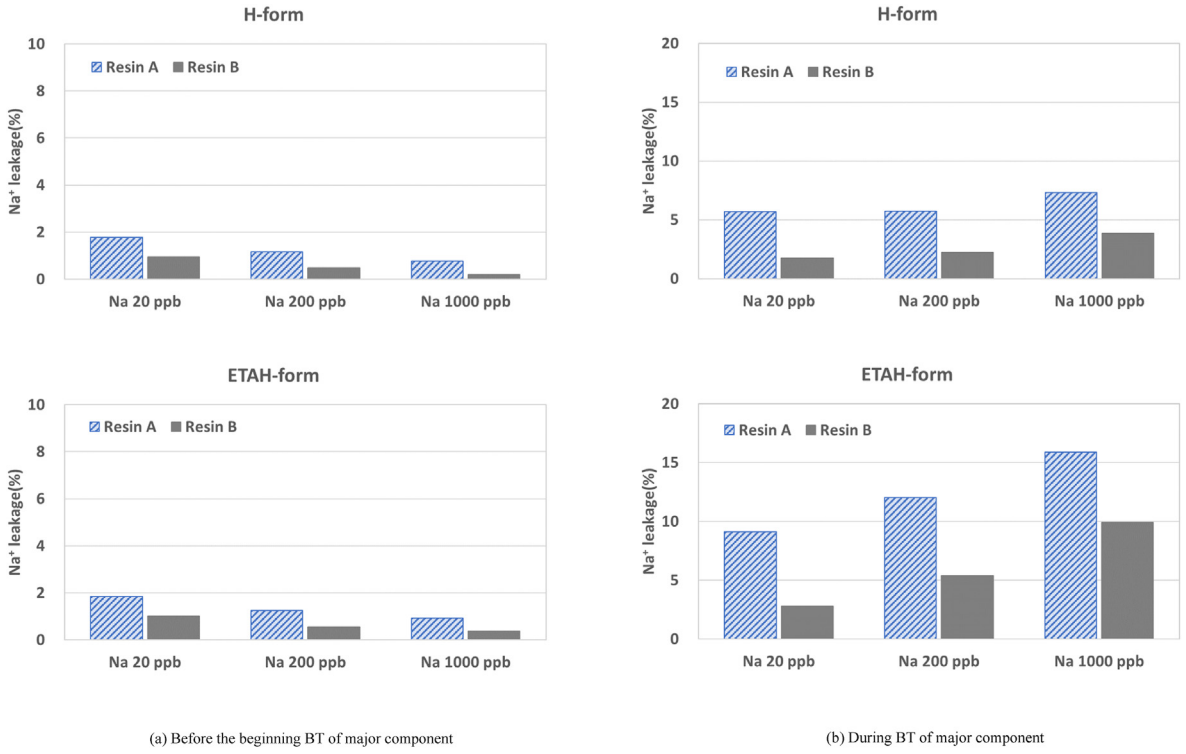

Fig. 3. Na^+ leakage from mixed-IX bed of H- and ETAH-from with resin A and B at incoming Na concentrations of 20, 200 and 1000 ppb before and during BT of major component (at 25 °C, pH 10, 120 BV/hr).

the selectivity decreased by increasing the ionic strength of the solution may surpass that increased by decreasing its fraction. On other hands, the selectivity of the minor component is reduced more than that of the major component owing to the increases in ionic strength as well as its fraction, which results in the earlier and broader breakthrough for the minor component.

4.2.2. Dependence of Na^+ leakage on selectivity and mole fraction

Table 4 shows the simulated mole fractions of components in the solution and resin phases (saturated) at equilibrium by using Vanselow IX equation, based on the experimental data presented in Fig. 1. At the respective mole fractions of 0.064, 45.97, and 53.97% for Na^+, NH_4^+ and $ETAH^+$ in the feed solution, their selectivities are 8, 1.8, and 1.3 and their mole fractions are 0.33, 53.93, and 45.73% in the resin phase. The ratios in the mole fraction between the solution and solid phases are 5.21, 1.17, and 0.85. The release of Na^+ from the bed is delayed rather than major components because the breakthrough of an ion may be reached if the corresponding amount is flowed into the IX bed and selectively adsorbed onto the resin functional group. Na^+ at the mole fraction of 0.064% in influent may come close to its BT after the lapse of 6.1 (5.21:0.85) times the BT of $ETAH^+$ due to its higher selectivity to the resin functional group. That is, Na^+ may not accomplish the saturation if Na^+ may be not only still higher than major components for the individual ion-selectivity but also under-saturated at the resin phase, despite the decreasing selectivity with increasing Na^+ uptake.

The breakthrough of Na^+ may be earlier reached and wider spread by the increased mole faction of Na^+ in the feed solution from 20 (0.064) to 200 (0.64) and 1000 ppb (3.2%) due to the decreased selectivity of Na^+ as illustrated in Table 2. Na^+ leakage is increased from the beginning of BT for main component due to decreasing the selectivity of Na^+ with increasing the portions of ETAH-form and Na-form resins. Thus Na^+ leakage is earlier and more significant for the higher concentration of incoming Na^+. Na^+ leakage at the higher concentration of Na^+ in influent is represented by the BT curve with lower slope at earlier BT time.

It is not still understood with the chemical property (selectivity) that trace Na^+ was escaped from the IX bed at the early stage of its operation and that Na leakage was the lower for resin B regardless of its lower selectivity to Na^+.

Table 4
Simulated mole fractions of components in the solution and resin phases (saturated).

		Na^+			NH_4^+			$ETAH^+$		
Selectivity coefficient		**8**	7	6	1.8	1.78	1.75	1.3	1.29	1.27
Fraction (%)	Solution phase	**0.064**	0.64	3.20	45.97	45.68	44.40	53.97	53.68	52.40
	Resin phase	**0.33**	2.89	10.87	53.93	52.45	48.01	45.73	44.66	41.12
Ratio		***5.21***	*4.52*	*3.40*	***1.17***	*1.15*	*1.08*	***0.85***	*0.83*	*0.78*

$$K_M = \frac{(R-M)(H^+)}{(R-H)(M^+)} \rightarrow \frac{f_{R-H}}{f_{H^+}} = \frac{1}{K_M}\frac{f_{R-M}}{f_{M^+}} \rightarrow \frac{1}{K_{Na}}\frac{f_{R-Na}}{f_{Na^+}} = \frac{1}{K_{NH4}}\frac{f_{R-NH4}}{f_{NH4^+}} = \frac{1}{K_{ETAH}}\frac{f_{R-ETAH}}{f_{ETAH^+}}$$

$$f_{R-Na} + f_{R-NH4} + f_{R-ETAH} = 100\%$$

4.3. Dependence of Na leakage on physical property of resin (particle size)

Cation exchange process with a solution flowing down the resin bed is defined as the stoichiometric exchange between cations adsorbed and accessed on the negative-charge sites of a resin surface. The IX bed is packed with the huge number of resin particles that possess the intrinsic properties as shown in Table 1. Cations entered in the adsorption zone of the resin layer may be spread into intra-particle pore and inter-particle void proportionally to their volume fractions [13,14,16–18]. Cations are respectively captured on the negative-charge sites through the competition with other cations in the intra-particle pore and delivered to the adjoining zone through the inter-particle void. The inter-particle void in the top of the resin layer in IX bed is inter-connected to the bottom of the resin layer, resulting in a complicated channel [13,14,19–21]. It subsequently provides the escape pathway of a very small portion of ions to be released out of the IX bed shortly after the beginning of IX operation without ion exchange as mentioned earlier in section 4.1.

The dynamic IX process in the resin bed may depend on the void surrounded by particles and the selectivity of the IX resin to ions. The higher adsorption arises from less spreading to the inter-particle void in the resin layer and stronger uptake onto the exchange site in the bead. The IX resin of smaller size does not enhance only the dynamic IX process due to the increased number of particles packed in IX bed horizontally and vertically, but also the decreased volume of the inter-particle void created in the resin layer. Resin B was lowest for the selectivity to Na^+ (resin B < D≪A ≤ C) as well as for the particle size (resin B≪C < D≪A), which results in the contradicting impact on Na uptake. Resin B was lowest in the order of Na^+ leakage (resin B < A ≤ C < D) which is the similar sequence as the particle size. The experimental observation in section 4.1 suggests that the leakage of trace Na out of IX bed is predominantly influenced by particle size than selectivity.

The quantitative comparison of four kinds of IX resins was made with the volumes of pore and void and the numbers of resin particles in IX bed of spherical resin beads with face-centered cubic packing in Table 5. Since resin B is ~29% smaller than resin A in size and ~64% smaller in a void formed by surrounding particles, the numbers particles of resin B are needed ~2 times than those of resin A (used in existing NPP) to create the single resin layer with the same planar arrangements. Four kinds of resins are not big different in the porosity which consequently is not the critical parameter to evaluate the ion exchange performance including the characteristic of Na^+ leakage for the dynamic IX process.

It is reasonably derived that Na leakage depends absolutely on the particle size among the physical and chemical properties such as cation exchange capacity and ion selectivity. Meanwhile, the very small amounts of ions are escaped from the resin layer throughout the entire void in the inter-particle region (i.e., channel) from the beginning of IX operation without ion exchange.

5. Summary and conclusions

The physical and chemical properties of four kinds of resins such as particle size, density, void volume, porosity, cation exchange capacity, and selectivity coefficient were investigated through ASTM and experimental tests to obtain the mechanistic understanding of the leakage of a trace of Na from IX bed in the simulated waster-steam cycle of mixed ammonia and ethanolamine solution including trace NaCl.

The leakage of Na^+ insignificantly present in the simulated water-steam cycle was lowest from IX bed filled with resin B. The average selectivity was maintained in the increasing order of H^+ < $ETAH^+$ < Na^+ < NH_4^+ toward four resins and in the increasing order of resin B < D≪A ≤ C towards four cations. However, the affinity of a cation was increased with decreasing its fraction in the solution and decreased with increasing its adsorption on the exchange sites. Thus, the individual ion-selectivity may be decreased in the order of Na^+ > NH_4^+ > $ETAH^+$ > H^+ (> 2 for Na, < 1.8 for NH_4^+, < 1.3 for $ETAH^+$) at the cation composition of the feed solution with the major components of 45–55% (NH_4^+ and $ETAH^+$) and the minor component (Na^+) at 0.064, 0.64, and 3.2%. Mass action model of Vanselow equation for resin B exhibited better accuracy in predicting binary cation exchange. The resin B of gel-type was lowest in particle size and selectivity and was not remarkably different in backwashed & settled density and total cation exchange capacity from other resins.

With increasing cation coverage on the resin surfaces, cation selectivity was so decreased that Na leakage from the resin bed kept non-linearly increasing. Na^+ did not approach its breakthrough point even long after BT of major component if it is still higher than NH_4^+ as well as $ETAH^+$ for the selectivity to the cation-exchange resin due to less Na^+ uptake than its amount saturated at the feed composition. Na^+ leakage was larger from IX bed filled with R-ETAH resin than with R–H resin because the selectivity of Na^+ to $ETAH^+$ is lower than to H^+. Trace Na^+ could be escaped from the resin layer of IX bed throughout the channel, i.e., space surrounded by resin beads connected from the top to bottom of the resin layer, which was lowest for resin B of smallest size (resin B≪C < D≪A), contrarily to expectations with its lowest selectivity to Na. Thus, the particle size played a dominant role in the Na leakage rather than selectivity.

Table 5
Calculated Properties of Spherical Resin Beads packed in Face-Centered Cubic Structure (at 25 °C).

Properties		Type of resin			
		A	B	C	D
Moisture content (%)		34.36	36.24	41.57	51.89
Backwashed & settled density (g/mL)		1.93	1.65	1.81	1.85
Particle size (diameter, μm)		602	429	520	545
Volume (10^{-5} μm^3)	a sphere	11.42	4.13	7.36	8.47
	a void surrounded by particles	**4.01**	**1.45**	**2.58**	**2.97**
	pore inside a particle	8.85	2.81	6.41	9.44
	space (void + pore) per particle	12.86	4.26	8.99	12.42
Mass (10^{-4} g)	wet resin	103.0	31.0	61.6	72.8
	dried resin	67.6	19.8	36.0	35.0
Porosity (%)	pore-to-particle ratio in volume	**0.69**	**0.66**	**0.71**	**0.76**
Relative ratio	number of particles in a single layer	**0.51**	**1.00**	**0.68**	**0.62**
Density (g/mL)	wet resin	2.26	1.88	2.09	2.15
	dried resin	1.48	1.20	1.22	1.03

It is concluded that the particle size is the most important factor among the physical and chemical properties of IX resin to reduce Na^+ leakage from condensate polishing plants in the secondary system of nuclear power plants and in the ultrapure-water generation of such industries as electric power and electronics.

Declaration of competing interest

The authors declare that they have no known competing financial interests or personal relationships that could have appeared to influence the work reported in this paper.

Acknowledgments

This research was supported by Soonchunhyang University, Korea Hydro & Nuclear Power Central Research Institute (Grant No. L17S099001) and Korea Institute of Energy Technology Evaluation and Planning (Grant No. 20184030202130).

References

[1] K. Fruzzetti, Pressurized water reactor secondary water chemistry guideline, EPRI, Revision 6 (2006), 2-1-2-3.
[2] T. Fukumura, K. Arioka, Influence of ETA injection on flow accelerated corrosion of PWR secondary system, in: NACE Corrosion 2009 International Conference & Expo, NACE, U.S.A., 2009. March 22-26.
[3] C. Marks, Amine effect on corrosion product transports and steam generator fouling, in: Steam Generator Management Program 2010 Steam Generator Secondary Side Management Conference, EPRI, U.S.A., 2010. March 2-4.
[4] I.H. Rhee, Selection parameters for secondary pH control agent in PWR, in: Steam Generator Management Program 2010 Steam Generator Secondary Side Management Conference, EPRI, U.S.A., 2010. March 2-4.
[5] I.H. Rhee, Water quality of NPP secondary side with combined water chemistry of ammonia and ethanolamine, in: International Conference NPC, France, 23–28, 2012. September.
[6] I.H. Rhee, H.J. Jung, D.C. Cho, Evaluation of pH control agents influencing on corrosion of carbon steel in secondary water chemistry condition of pressurized water reactor, NET 46 (2014) 431–438.
[7] Y.B. Lee, J.M. Lee, D.H. Hur, J.H. Lee, S.H. Jeon, Effects of advanced amines on magnetite deposition of steam generator tubes in secondary system, Coatings 514 (2021) 1–19.
[8] H.K. Ahn, Y.S. Kim, B.G. Park, I.H. Rhee, A study on breakthrough characteristics of ion exchange bed with H- and ETAH-form resins for cation exchange in NH3 and ETA solution including trace NaCl, J. Kor. Soc. Water Wastewater 35 (2021) 533–544.
[9] W. Bashir, E. Tyrrell, O. Feeney, B. Paull, Retention of alkali, alkaline earth and transition metals on an itaconic acid cation-exchange column: eluent pH, ionic strength and temperature effects upon selectivity, J. Chromatogr A 964 (2002) 113–122.
[10] M.B. Richard, K. Jacek, Ion exchange selectivity and electrolyte concentration, J. Chem. Soc., Faraday Trans. 1 (1974) 70, 2080-2091.
[11] ASTM, Standard Test Methods and Practices for Evaluating Physical and Chemical Properties of Particulate Ion-Exchange Resins1, 2017. ASTM D2187-17.
[12] I.H. Rhee, D.A. Dzombak, Binary and ternary cation exchange on strong acid cation exchange resin involving Na, Mg, and Zn in single and binary backgrounds of chloride, perchlorate, and sulfate, Langmuir 15 (1999) 6875–6883.
[13] F.P. Reinhard, Utilization and practical application of ion exchange, A critical review, in: 14th Annual AESF/EPA Conference on Environmental Control for the Surface Finishing Industry, 26–28, EPA, U.S.A., 1993. January.
[14] I. Curran Woodard, Industrial Waste Treatment Handbook, second ed., Butterworth-Heinemann, 2005.
[15] B.S. Salem, A.S. Asli, O. Ahmet, Fixed-bed ion exchange columns operating under non-equilibrium conditions: estimation of mass transfer properties via non-equilibrium modeling, React. Funct. Polym. 67 (12) (2007) 1540–1547.
[16] E.L. Alfredo, Diffusion in Ion-Exchange Resins, Ph.D dissertation, University of London, U.K, 1960.
[17] K.P. Sudhir, Mixed Bed Ion-Exchange Modeling for Divalent Ions in a Ternary System, Ph.D dissertation, Andhra University, India, 1992.
[18] A.N. Valentina, About mathematical modeling and calculation of dynamic ion-exchange processes on natural zeolites, in: Handbook of Natural Zeolites, Bentham Science Pub, 2012, pp. 452–472.
[19] V.H. Fabíola, G. Franciélle, C.S. João, Antônio Augusto U. de Souza, Rui A.R. Boaventura, Selene M.A. Guelli U. de Souza, Vítor J.P. Vilar, Ion-exchange breakthrough curves for single and multi-metal systems using marine macroalgae Pelvetia canaliculata as a natural cation exchanger, Chem. Eng. J. 269 (2015) 359–370.
[20] J. Yi, L.F. Gary, True multi-component mixed-bed ion-exchange modeling, React. Funct. Polym. 60 (2004) 121–135.
[21] S. Fisher, F.X. McGarvey, Ion Exchange Technology in the Nuclear Fuel Cycle, International Atomic Energy Agency, Vienna, 1986, pp. 9–52. IAEA-TECDOC-365.